# Atmosphere Modeling: Dynamics I

## the CAM (Community Atmosphere Model) FV (Finite Volume) dynamical core

Peter Hjort Lauritzen

Atmospheric Modeling and Predictability Section (AMP)
Climate and Global Dynamics Division (CGD)
NCAR Earth System Laboratory (NESL)
National Center for Atmospheric Research (NCAR)

Summer school: Introduction to Climate Modeling (University of Stockholm)

1. Atmosphere intro
   - Multi-scale nature of atmosphere dynamics
   - Resolved and un-resolved scales
   - 'Define' dynamical core and parameterizations

2. CAM-FV dynamical core (current default core)
   - Horizontal and vertical grid
   - Equations of motion
   - The Lin and Rood (1996) advection scheme
   - Finite-volume discretization of the equations of motion
   - The 'CD' grid approach
   - Vertical remapping
   - Tracers
   - Known problems ('features')

3. Other dynamical core options in CAM

# Domain

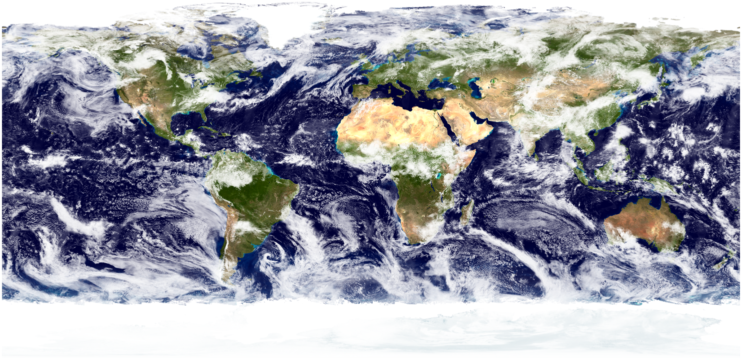

Source: NASA Earth Observatory

# Horizontal computational space

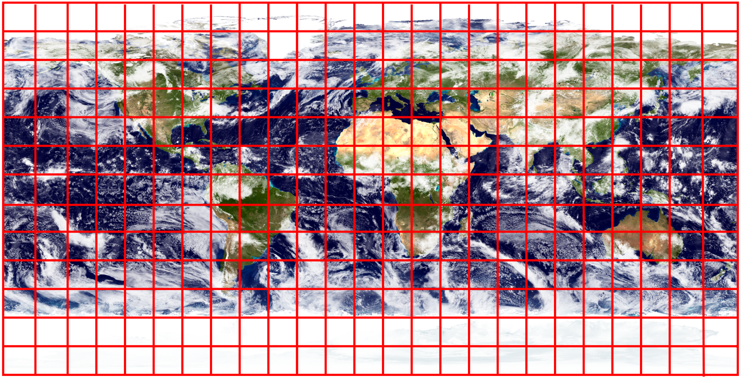

- Red lines: Regular latitude-longitude grid
- Grid-cell size defines the smallest scale that can be resolved
- Many important processes taking place sub-grid-scale that must be parameterized
- Loosely speaking, the parameterizations compute grid-cell average tendencies due to sub-grid-scale processes in terms of the (resolved scale) atmospheric state
- In modeling jargon parameterizations are also referred to as *physics* (what is unphysical about resolved scale dynamics?)

# Multi-scale nature of atmosphere dynamics (from Thuburn 2011)

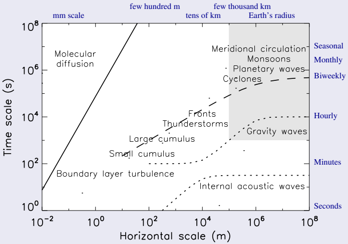


Figure indicates schematically the time scales and horizontal spatial scales of a range of atmospheric phenomena (Figure from Thuburn 2011).

# Multi-scale nature of atmosphere dynamics (from Thuburn 2011)

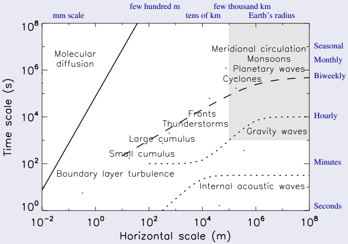


Figure indicates schematically the time scales and horizontal spatial scales of a range of atmospheric phenomena (Figure from Thuburn 2011).

- $\mathcal{O}(10^4\,km)$: Large scale circulations (Asian summer monsoon).

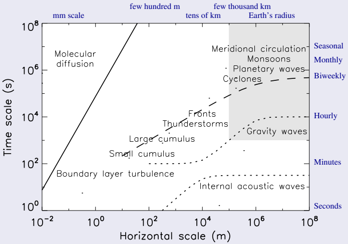


Figure indicates schematically the time scales and horizontal spatial scales of a range of atmospheric phenomena (Figure from Thuburn 2011).

- $\mathcal{O}(10^4 km)$: Large scale circulations (Asian summer monsoon).
- $\mathcal{O}(10^4 km)$: Undulations in the jet stream and pressure patterns associated with the largest scale Rossby waves (called *planetary waves*)

# Multi-scale nature of atmosphere dynamics (from Thuburn 2011)

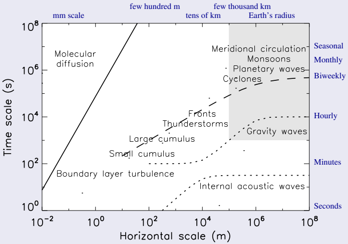


Figure indicates schematically the time scales and horizontal spatial scales of a range of atmospheric phenomena (Figure from Thuburn 2011).

- $\mathcal{O}(10^4 km)$: Large scale circulations (Asian summer monsoon).
- $\mathcal{O}(10^4 km)$: Undulations in the jet stream and pressure patterns associated with the largest scale Rossby waves (called *planetary waves*)
- $\mathcal{O}(10^3 km)$: Cyclones and anticyclones

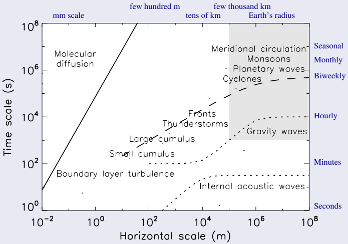


Figure indicates schematically the time scales and horizontal spatial scales of a range of atmospheric phenomena (Figure from Thuburn 2011).

- $\mathcal{O}(10^4 km)$: Large scale circulations (Asian summer monsoon).
- $\mathcal{O}(10^4 km)$: Undulations in the jet stream and pressure patterns associated with the largest scale Rossby waves (called *planetary waves*)
- $\mathcal{O}(10^3 km)$: Cyclones and anticyclones
- $\mathcal{O}(10 km)$: The transition zones between relatively warm and cool air masses can collapse in scale to form fronts with widths of a few tens of $\mathrm{km}$

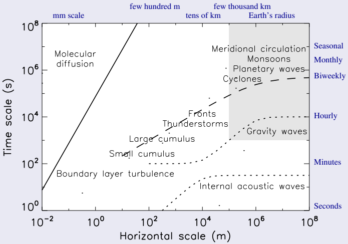


Figure indicates schematically the time scales and horizontal spatial scales of a range of atmospheric phenomena (Figure from Thuburn 2011).

- $\mathcal{O}(10^4 km)$: Large scale circulations (Asian summer monsoon).
- $\mathcal{O}(10^4 km)$: Undulations in the jet stream and pressure patterns associated with the largest scale Rossby waves (called *planetary waves*)
- $\mathcal{O}(10^3 km)$: Cyclones and anticyclones
- $\mathcal{O}(10 km)$: The transition zones between relatively warm and cool air masses can collapse in scale to form fronts with widths of a few tens of km
- $\mathcal{O}(10^3 km - 100 m)$: Convection can be organized on a huge range of different scales (tropical intraseasonal oscillations; supercell complexes and squall lines; individual small cumulus clouds formed from turbulent boundary layer eddies)

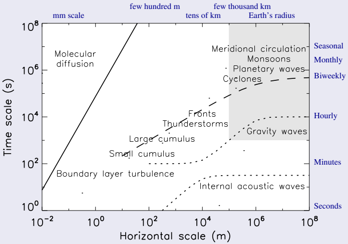


Figure indicates schematically the time scales and horizontal spatial scales of a range of atmospheric phenomena (Figure from Thuburn 2011).

- $\mathcal{O}(10^4 km)$: Large scale circulations (Asian summer monsoon).
- $\mathcal{O}(10^4 km)$: Undulations in the jet stream and pressure patterns associated with the largest scale Rossby waves (called *planetary waves*)
- $\mathcal{O}(10^3 km)$: Cyclones and anticyclones
- $\mathcal{O}(10 km)$: The transition zones between relatively warm and cool air masses can collapse in scale to form fronts with widths of a few tens of km
- $\mathcal{O}(10^3 km - 100 m)$: Convection can be organized on a huge range of different scales (tropical intraseasonal oscillations; supercell complexes and squall lines; individual small cumulus clouds formed from turbulent boundary layer eddies)
- $\mathcal{O}(10 m - 1 mm)$: Turbulent eddies in boundary layer (lowest few hundred *m*'s of the atmosphere, where the dynamics is dominated by turbulent transports); range in scale from few hundred *m*'s (the boundary layer depth) down to *mm* scale at which molecular diffusion becomes significant.

# Multi-scale nature of atmosphere dynamics (from Thuburn 2011)

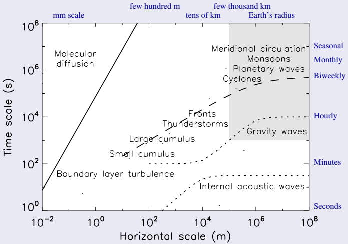


- All of the phenomena along the dashed line are important for weather and climate, and so need to be represented in numerical models.
- Important phenomena occur at all scales - there is no significant *spectral gap*! Moreover, there are strong interactions between the phenomena at different scales, and these interactions need to be represented.
- The lack of any spectral gap makes the modeling of weather/climate very challenging
- The emphasis in this lecture is how we model resolved dynamics; however, it should be borne in mind that equally important is how we represent unresolved processes, and the interactions between resolved and unresolved processes.

- $\mathcal{O}(10^4\,km)$: Large scale circulations (Asian summer monsoon).
- $\mathcal{O}(10^4\,km)$: Undulations in the jet stream and pressure patterns associated with the largest scale Rossby waves (called *planetary waves*)
- $\mathcal{O}(10^3\,km)$: Cyclones and anticyclones
- $\mathcal{O}(10km)$: The transition zones between relatively warm and cool air masses can collapse in scale to form fronts with widths of a few tens of $\mathrm{km}$
- $\mathcal{O}(10^3\,km - 100m)$: Convection can be organized on a huge range of different scales (tropical intraseasonal oscillations; supercell complexes and squall lines; individual small cumulus clouds formed from turbulent boundary layer eddies)
- $\mathcal{O}(10m - 1mm)$: Turbulent eddies in boundary layer (lowest few hundred *m*'s of the atmosphere, where the dynamics is dominated by turbulent transports); range in scale from few hundred *m*'s (the boundary layer depth) down to *mm* scale at which molecular diffusion becomes significant.

# Multi-scale nature of atmosphere dynamics (from Thuburn 2011)

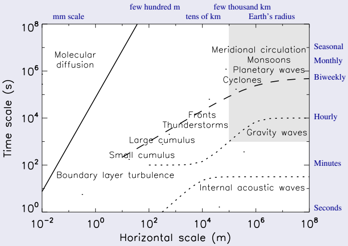


- Two dotted curves correspond to dispersion relations for internal inertio-gravity waves and internal acoustic waves (relatively fast processes)
- these lines lie significantly below the energetically dominant processes on the dashed line
  - $\Rightarrow$ they are energetically weak compared to the dominant processes along the dashed curve
  - $\Rightarrow$ we do relatively little damage if we distort their propagation (will return to this later)
  - the fact that these waves are fast puts strong constraints on $\Delta t$ that can be used in numerical models with explicit time schemes.

- $\mathcal{O}(10^4 km)$: Large scale circulations (Asian summer monsoon).
- $\mathcal{O}(10^4 km)$: Undulations in the jet stream and pressure patterns associated with the largest scale Rossby waves (called *planetary waves*)
- $\mathcal{O}(10^3 km)$: Cyclones and anticyclones
- $\mathcal{O}(10 km)$: The transition zones between relatively warm and cool air masses can collapse in scale to form fronts with widths of a few tens of km
- $\mathcal{O}(10^3 km - 100 m)$: Convection can be organized on a huge range of different scales (tropical intraseasonal oscillations; supercell complexes and squall lines; individual small cumulus clouds formed from turbulent boundary layer eddies)
- $\mathcal{O}(10 m - 1 mm)$: Turbulent eddies in boundary layer (lowest few hundred $m$'s of the atmosphere, where the dynamics is dominated by turbulent transports); range in scale from few hundred $m$'s (the boundary layer depth) down to $mm$ scale at which molecular diffusion becomes significant.

# Multi-scale nature of atmosphere dynamics (from Thuburn 2011)

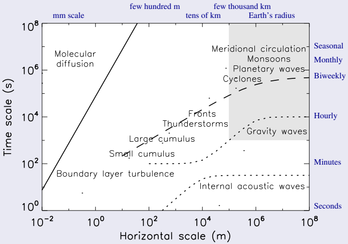


Horizontal resolution:

- The shaded region shows the resolved space/time scales in typical current day climate models (approximately $1^\circ - 2^\circ$ resolution)
- Highest resolutions at which CAM has been run is on the order of $10 - 25km$
- As the resolution is increased some 'large-scale' parameterizations may no longer be necessary (e.g., large scale convection) and we might need to redesign some parameterizations that were developed for horizontal resolutions of hundreds of km's

- $\mathcal{O}(10^4 km)$: Large scale circulations (Asian summer monsoon).
- $\mathcal{O}(10^4 km)$: Undulations in the jet stream and pressure patterns associated with the largest scale Rossby waves (called *planetary waves*)
- $\mathcal{O}(10^3 km)$: Cyclones and anticyclones
- $\mathcal{O}(10 km)$: The transition zones between relatively warm and cool air masses can collapse in scale to form fronts with widths of a few tens of km
- $\mathcal{O}(10^3 km - 100m)$: Convection can be organized on a huge range of different scales (tropical intraseasonal oscillations; supercell complexes and squall lines; individual small cumulus clouds formed from turbulent boundary layer eddies)
- $\mathcal{O}(10m - 1mm)$: Turbulent eddies in boundary layer (lowest few hundred $m$'s of the atmosphere, where the dynamics is dominated by turbulent transports); range in scale from few hundred $m$'s (the boundary layer depth) down to $mm$ scale at which molecular diffusion becomes significant.

# Multi-scale nature of atmosphere dynamics (from Thuburn 2011)

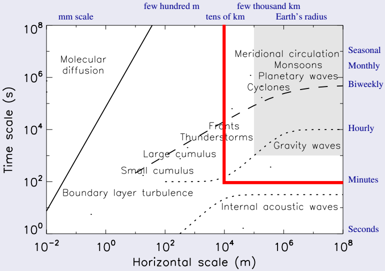


Horizontal resolution:

- The shaded region shows the resolved space/time scales in typical current day climate models (approximately $1^{\circ} - 2^{\circ}$ resolution)
- Highest resolutions at which CAM has been run is on the order of $10 - 25km$
- As the resolution is increased some 'large-scale' parameterizations may no longer be necessary (e.g., large scale convection) and we might need to redesign some parameterizations that were developed for horizontal resolutions of hundreds of km's

- $\mathcal{O}(10^4 km)$: Large scale circulations (Asian summer monsoon).
- $\mathcal{O}(10^4 km)$: Undulations in the jet stream and pressure patterns associated with the largest scale Rossby waves (called *planetary waves*)
- $\mathcal{O}(10^3 km)$: Cyclones and anticyclones
- $\mathcal{O}(10 km)$: The transition zones between relatively warm and cool air masses can collapse in scale to form fronts with widths of a few tens of km
- $\mathcal{O}(10^3 km - 100m)$: Convection can be organized on a huge range of different scales (tropical intraseasonal oscillations; supercell complexes and squall lines; individual small cumulus clouds formed from turbulent boundary layer eddies)
- $\mathcal{O}(10m - 1mm)$: Turbulent eddies in boundary layer (lowest few hundred *m*'s of the atmosphere, where the dynamics is dominated by turbulent transports); range in scale from few hundred *m*'s (the boundary layer depth) down to *mm* scale at which molecular diffusion becomes significant.

# Model code

## Parameterization suite

- Moist processes: Deep convection, shallow convection, large-scale condensation
- Radiation and Clouds: Cloud microphysics, precipitation processes, radiation
- Turbulent mixing: Planetary boundary layer parameterization, vertical diffusion, gravity wave drag

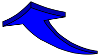

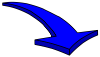

## 'Resolved' dynamics

'Roughly speaking, the **dynamical core** solves the governing fluid and thermodynamic equations on resolved scales, while the parameterizations represent sub-grid-scale processes and other processes not included in the dynamical core such as radiative transfer.' - Thuburn (2008)

# Model code

## Parameterization suite

- Moist processes: Deep convection, shallow convection, large-scale condensation
- Radiation and Clouds: Cloud microphysics, precipitation processes, radiation
- Turbulent mixing: Planetary boundary layer parameterization, vertical diffusion, gravity wave drag

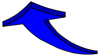

Strategies for coupling:

- process-split: dynamical core & parameterization suite are based on the same state and their tendencies are added to produce the updated state (used in CAM-EUL)
- time-split: dynamic core & parameterization suite are calculated sequentially, each based on the state produced by the other (used in CAM-FV; the order matters!).
- different coupling approaches discussed in the context CCM3 in Williamson (2002)
- simulations are very dependent on coupling time-step (e.g. Williamson and Olson, 2003)

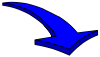

## 'Resolved' dynamics

'Roughly speaking, the **dynamical core** solves the governing fluid and thermodynamic equations on resolved scales, while the parameterizations represent sub-grid-scale processes and other processes not included in the dynamical core such as radiative transfer.' - Thuburn (2008)

# Spherical (horizontal) discretization grid

CAM-FV uses regular latitude-longitude grid:

- Horizontal position: $(\lambda, \theta)$, where $\lambda$ longitude and $\theta$ latitude.
- Horizontal resolution specified in `configure` as:

$$\texttt{-res}\ \Delta\lambda \times \Delta\theta$$

where, e.g., $\Delta\lambda \times \Delta\theta = 1.9 \times 2.5$ corresponding to `nlon=144, nlat=96`.

Changing resolution requires a 're-compile' .

- CAM-FV uses a Lagrangian ('floating') vertical coordinate $\xi$ so that

$$\frac{d\xi}{dt} = 0,$$

i.e. vertical surfaces are material surfaces (no flow across them).

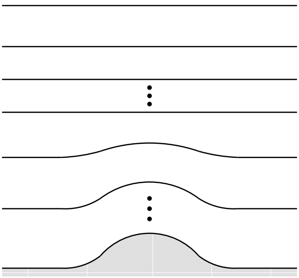

Figure shows 'usual' hybrid $\sigma - p$ vertical coordinate $\eta(p_s, p)$ (where $p_s$ is surface pressure):

- $\eta(p_s, p)$ is a monotonic function of $p$.
- $\eta(p_s, p_s) = 1$
- $\eta(p_s, 0) = 0$
- $\eta(p_s, p_{top}) = \eta_{top}$.

Boundary conditions are:

- $\frac{d\eta(p_s,p_s)}{dt} = 0$
- $\frac{d\eta(p_s,p_{top})}{dt} = \omega(p_{top}) = 0$

($\omega$ is vertical velocity in pressure coordinates)

- CAM-FV uses a Lagrangian ('floating') vertical coordinate $\xi$ so that

$$\frac{d\xi}{dt} = 0,$$

i.e. vertical surfaces are material surfaces (no flow across them).

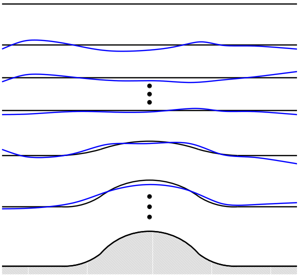

Figure:

- Set $\xi = \eta$ at time $t_{start}$ (black lines).
- For $t > t_{start}$ the vertical levels deform as they move with the flow (blue lines).
- To avoid excessive deformation of the vertical levels (non-uniform vertical resolution) the prognostic variables defined in the Lagrangian layers $\xi$ are periodically remapped (= conservative interpolation) back to the Eulerian reference coordinates $\eta$ (more on this later).

# Vertical coordinate

- Vertical resolution specified in `configure` as:

`-nlev` *klev*

where *klev* is the number of vertical levels, e.g., $klev = 26$ or $klev = 30$. Changing vertical resolution requires a 're-compile'.

The vertical extent is from the surface to

- approximately 40 km's / 2hPa for CAM
- approximately 100 km's / $10^{-6}$ hPa for WACCM (Whole Atmosphere Community Climate Model)
- approximately 500 km's / $10^{-9}$ hPa for WACCM-x

# Adiabatic frictionless equations of motion

The following approximations are made to the compressible Euler equations:

- **Spherical geoid**: Geopotential $\Phi$ is only a function of radial distance from the center of the Earth $r$: $\Phi = \Phi(r)$ (for planet Earth the true gravitational acceleration is much stronger than the centrifugal force).
  $\Rightarrow$ Effective gravity acts only in radial direction

The following approximations are made to the compressible Euler equations:

- **Spherical geoid**: Geopotential $\Phi$ is only a function of radial distance from the center of the Earth $r$: $\Phi = \Phi(r)$ (for planet Earth the true gravitational acceleration is much stronger than the centrifugal force).
  $\Rightarrow$ Effective gravity acts only in radial direction
- **Quasi-hydrostatic approximation** (also simply referred to as *hydrostatic approximation*): Involves ignoring the acceleration term in the vertical component of the momentum equations so that it reads:

$$\rho\, g = -\frac{\partial p}{\partial z}, \qquad (1)$$

  where $g$ gravity, $\rho$ density and $p$ pressure. Good approximation down to horizontal scales greater than approximately $10km$.

The following approximations are made to the compressible Euler equations:

- **Spherical geoid**: Geopotential $\Phi$ is only a function of radial distance from the center of the Earth $r$: $\Phi = \Phi(r)$ (for planet Earth the true gravitational acceleration is much stronger than the centrifugal force).
  $\Rightarrow$ Effective gravity acts only in radial direction
- **Quasi-hydrostatic approximation** (also simply referred to as *hydrostatic approximation*): Involves ignoring the acceleration term in the vertical component of the momentum equations so that it reads:

$$\rho g = -\frac{\partial p}{\partial z}, \qquad (1)$$

  where $g$ gravity, $\rho$ density and $p$ pressure. Good approximation down to horizontal scales greater than approximately $10km$.
- **Shallow atmosphere**: A collection of approximations. Coriolis terms involving the horizontal components of $\Omega$ are neglected ($\Omega$ is angular velocity), factors $1/r$ are replaced with $1/a$ where $a$ is the mean radius of the Earth and certain other metric terms are neglected so that the system retains conservation laws for energy and angular momentum.

# Adiabatic frictionless equations of motion using Lagrangian vertical coordinates

Assuming a Lagrangian vertical coordinate the hydrostatic equations of motion integrated over a layer can be written as

$$\begin{aligned}
\text{mass air:} \quad & \frac{\partial(\delta p)}{\partial t} = -\nabla_h \cdot (\vec{v}_h \delta p)\,, \\
\text{mass tracers:} \quad & \frac{\partial(\delta p q)}{\partial t} = -\nabla_h \cdot (\vec{v}_h\, q \delta p)\,, \\
\text{horizontal momentum:} \quad & \frac{\partial \vec{v}_h}{\partial t} = -(\zeta + f)\,\vec{k} \times \vec{v}_h - \nabla_h \kappa - \nabla_p \Phi, \\
\text{thermodynamic:} \quad & \frac{\partial(\delta p \Theta)}{\partial t} = -\nabla_h \cdot (\vec{v}_h \delta p \Theta)
\end{aligned}$$

where $\delta p$ is the layer thickness, $\vec{v}_h$ is horizontal wind, $q$ tracer mixing ratio, $\zeta$ vorticity, $f$ Coriolis, $\kappa$ kinetic energy, $\Theta$ potential temperature. The momentum equations are written in vector invariant form.

# Adiabatic frictionless equations of motion using Lagrangian vertical coordinates

Assuming a Lagrangian vertical coordinate the hydrostatic equations of motion integrated over a layer can be written as

$$
\begin{aligned}
\text{mass air:} \quad & \frac{\partial(\delta p)}{\partial t} = -\nabla_h \cdot (\vec{v}_h \delta p)\,, \\
\text{mass tracers:} \quad & \frac{\partial(\delta p q)}{\partial t} = -\nabla_h \cdot (\vec{v}_h\, q \delta p)\,, \\
\text{horizontal momentum:} \quad & \frac{\partial \vec{v}_h}{\partial t} = -(\zeta + f)\, \vec{k} \times \vec{v}_h - \nabla_h \kappa - \nabla_p \Phi, \\
\text{thermodynamic:} \quad & \frac{\partial(\delta p \Theta)}{\partial t} = -\nabla_h \cdot (\vec{v}_h \delta p \Theta)
\end{aligned}
$$

The equations of motion are discretized using an Eulerian finite-volume approach.

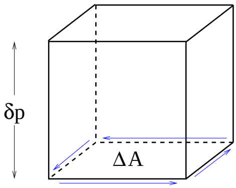


Integrate the flux-form continuity equation horizontally over a control volume:

$$\frac{\partial}{\partial t}\iint_A \delta p \, dA = -\iint_A \nabla_h \left(\vec{v}_h \delta p\right) \, dA, \tag{2}$$

where $A$ is the horizontal extent of the control volume. Using Gauss's divergence theorem for the right-hand side of (2) we get:

$$\frac{\partial}{\partial t}\iint_A \delta p \, dA = -\oint_{\partial A} \delta p \, \vec{v} \cdot \vec{n} \, dA, \tag{3}$$

where $\partial A$ is the boundary of $A$ and $\vec{n}$ is outward pointing normal unit vector of $\partial A$.

# Finite-volume discretization of continuity equation

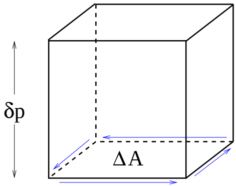


Integrate the flux-form continuity equation horizontally over a control volume:

$$\frac{\partial}{\partial t}\iint_A \delta p \, dA = -\iint_A \nabla_h \left(\vec{v}_h \delta p\right) \, dA, \tag{2}$$

where $A$ is the horizontal extent of the control volume. Using Gauss's divergence theorem for the right-hand side of (2) we get:

$$\frac{\partial}{\partial t}\iint_A \delta p \, dA = -\oint_{\partial A} \delta p \, \vec{v} \cdot \vec{n} \, dA, \tag{3}$$

Right-hand side of (3) represents the instantaneous flux of mass through the vertical faces of the control volume.

# Finite-volume discretization of continuity equation

$$\frac{\partial}{\partial t} \iint_A \delta p \, dA = -\oint_{\partial A} \delta p \, \vec{v} \cdot \vec{n} \, dA. \quad (4)$$

Discretize (4) in space

$$\Delta A \frac{\partial \overline{\delta p}}{\partial t} = -\sum_{f=1}^{4} \left[ \langle \delta p \vec{v} \rangle \cdot \vec{n} \Delta \ell \right]_f , \quad (5)$$

where

- $\overline{\delta} p$ = horizontal mean value of $\delta p$
- $\vec{n}_f$ = unit vector normal to the $f$th cell face pointing outward
- $\Delta \ell_f$ is the length of the face in question
- $\vec{v}_f$ = instantaneous values of $\vec{v}$ at the cell face $f$
- brackets represent averages in either $\lambda$ or $\theta$ direction over the cell face.

# Finite-volume discretization of continuity equation

$$\frac{\partial}{\partial t}\iint_A \delta p \, dA = -\oint_{\partial A} \delta p \, \vec{v}\cdot\vec{n}\, dA. \tag{4}$$

Discretize (4) in space

$$\Delta A \, \frac{\partial \overline{\delta p}}{\partial t} = -\sum_{f=1}^{4} \left[ \langle \delta p \vec{v} \rangle \cdot \vec{n} \Delta \ell \right]_f \, , \tag{5}$$

and integrate (5) over the time-step $\Delta t_{dyn}$

$$\Delta A \, \overline{\delta p}^{n+1} = \Delta A \, \overline{\delta p}^{n} - \Delta t_{dyn} \sum_{f=1}^{4} \left[ \overline{\overline{\langle \delta p \vec{v} \rangle}} \cdot \vec{n} \Delta \ell \right]_f \, , \tag{6}$$

where $n$ is the time-level index and the double-bar refers to the time average over $\Delta t_{dyn}$.

Each term in the sum on the right-hand side of (6) represents the mass transported through one of the four vertical control volume faces into the cell during one time-step (graphical illustration on next page).

# Finite-volume discretization of continuity equation: Tracking mass

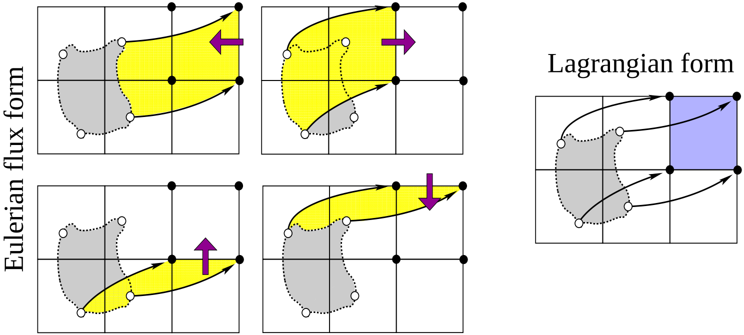


The yellow areas are 'swept' through the control volume faces during one time-step. The grey area is the corresponding Lagrangian area (area moving with the flow with no flow through its boundaries that ends up at the Eulerian control volume after one time-step). Black arrows show parcel trajectories.

Equivalence between Eulerian flux-form and Lagrangian form!

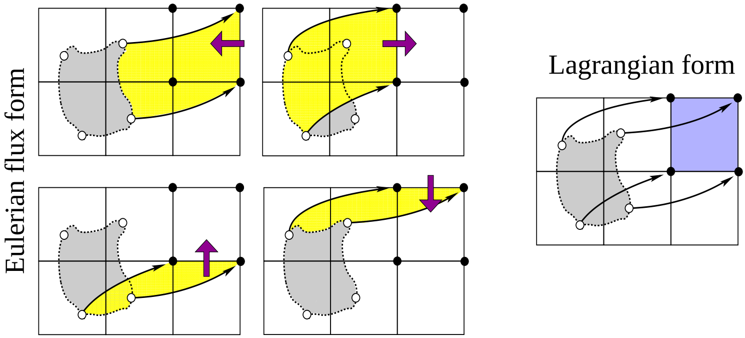


Until now everything has been exact. How do we approximate the fluxes numerically?

- In CAM-FV the Lin and Rood (1996) scheme is used which is a dimensionally split scheme (that is, rather than estimating the boundaries of the yellow areas and integrate over them, fluxes are estimated by successive applications of one-dimensional operators in each coordinate direction).

# Finite-volume discretization of continuity equation: Tracking mass

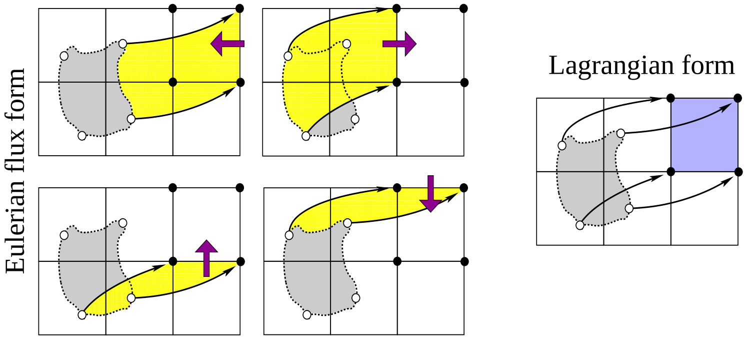


Until now everything has been exact. How do we approximate the fluxes numerically?

- (before showing equations for Lin and Rood (1996) scheme) What is the effective Lagrangian area associated with the Lin and Rood (1996) scheme?

# Finite-volume discretization of continuity equation: Tracking mass

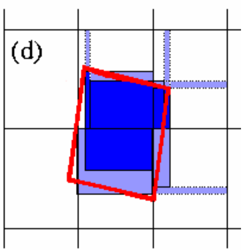


Figure: Red lines define boundary of exact Lagrangian cell for a special case with deformational, rotational and divergent wind field. Blue colors is Lagrangian cell associated with the Lin and Rood (1996) scheme. Dark blue shading weights integrated mass with 1 and light blue shading weights integrated mass with 1/2. See Machenhauer et al. (2009) for details.

Until now everything has been exact. How do we approximate the fluxes numerically?

- (before showing equations for Lin and Rood (1996) scheme) What is the effective Lagrangian area associated with the Lin and Rood (1996) scheme?

$$\overline{\delta p}^{n+1} = \overline{\delta p}^{n} + F^{\lambda}\left[\frac{1}{2}\left(\overline{\delta p}^{n} + f^{\theta}(\overline{\delta p}^{n})\right)\right] + F^{\theta}\left[\frac{1}{2}\left(\overline{\delta p}^{n} + f^{\lambda}(\overline{\delta p}^{n})\right)\right],$$

where

$$F^{\lambda,\theta} = \text{flux divergence in } \lambda \text{ or } \theta \text{ coordinate direction}$$

$$f^{\lambda,\theta} = \text{advective update in } \lambda \text{ or } \theta \text{ coordinate direction}$$

$$\overline{\delta p}^{n+1} = \overline{\delta p}^{n} + F^{\lambda}\left[\frac{1}{2}\left(\overline{\delta p}^{n} + f^{\theta}(\overline{\delta p}^{n})\right)\right] + F^{\theta}\left[\frac{1}{2}\left(\overline{\delta p}^{n} + f^{\lambda}(\overline{\delta p}^{n})\right)\right],$$

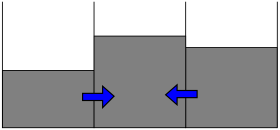

- Figure: Graphical illustration of flux-divergence operator $F^{\lambda}$. Shaded areas show cell average values for the cell we wish to make a forecast for and the two adjacent cells.

$$\overline{\delta p}^{n+1} = \overline{\delta p}^{n} + F^{\lambda}\left[\frac{1}{2}\left(\overline{\delta p}^{n} + f^{\theta}(\overline{\delta p}^{n})\right)\right] + F^{\theta}\left[\frac{1}{2}\left(\overline{\delta p}^{n} + f^{\lambda}(\overline{\delta p}^{n})\right)\right],$$

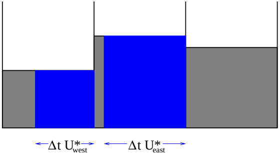


- $u^*_{east/west}$ are the time-averaged winds on each face (more on how these are obtained later).
- $F^{\lambda}$ is proportional to the difference between mass 'swept' through east and west cell face.
- $f^{\lambda} = F^{\lambda} + \overline{\overline{<\delta p>}}\Delta t_{dyn} D$, where $D$ is divergence.
- On Figure we assume constant sub-grid-cell reconstructions for the fluxes.

$$\overline{\delta p}^{n+1} = \overline{\delta p}^{n} + F^{\lambda}\left[\frac{1}{2}\left(\overline{\delta p}^{n} + f^{\theta}(\overline{\delta p}^{n})\right)\right] + F^{\theta}\left[\frac{1}{2}\left(\overline{\delta p}^{n} + f^{\lambda}(\overline{\delta p}^{n})\right)\right],$$

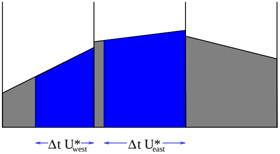


Higher-order approximation to the fluxes:

- Piecewise linear sub-grid-scale reconstruction (van Leer, 1977): Fit a linear function using neighboring grid-cell average values with mass-conservation as a constraint (i.e. area under linear function = cell average.).

$$\overline{\delta p}^{n+1} = \overline{\delta p}^{n} + F^{\lambda}\left[\frac{1}{2}\left(\overline{\delta p}^{n} + f^{\theta}(\overline{\delta p}^{n})\right)\right] + F^{\theta}\left[\frac{1}{2}\left(\overline{\delta p}^{n} + f^{\lambda}(\overline{\delta p}^{n})\right)\right],$$

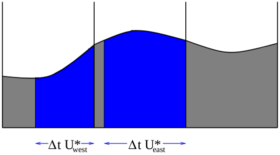


Higher-order approximation to the fluxes:

- Piecewise linear sub-grid-scale reconstruction (van Leer, 1977): Fit a linear function using neighboring grid-cell average values with mass-conservation as a constraint (i.e. area under linear function = cell average.).
- Piecewise parabolic sub-grid-scale reconstruction (Colella and Woodward, 1984): Fit parabola using neighboring grid-cell average values with mass-conservation as a constraint. Note: Reconstruction is $C^0$ across cell edges.

## The Lin and Rood (1996) advection scheme

$$\overline{\delta p}^{n+1} = \overline{\delta p}^{n} + F^{\lambda}\left[\frac{1}{2}\left(\overline{\delta p}^{n} + f^{\theta}(\overline{\delta p}^{n})\right)\right] + F^{\theta}\left[\frac{1}{2}\left(\overline{\delta p}^{n} + f^{\lambda}(\overline{\delta p}^{n})\right)\right],$$

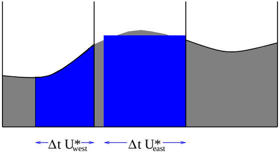


Higher-order approximation to the fluxes:

- Piecewise linear sub-grid-scale reconstruction (van Leer, 1977): Fit a linear function using neighboring grid-cell average values with mass-conservation as a constraint (i.e. area under linear function = cell average.).
- Piecewise parabolic sub-grid-scale reconstruction (Colella and Woodward, 1984): Fit parabola using neighboring grid-cell average values with mass-conservation as a constraint. Note: Reconstruction is continuous at cell edges.
- Reconstruction function may 'over'- or 'undershoot' which may lead to unphysical and/or oscillatory solutions. Use limiters to render reconstruction function shape-preserving.

# The Lin and Rood (1996) advection scheme

$$\overline{\delta p}^{n+1} = \overline{\delta p}^{n} + F^{\lambda}\left[\frac{1}{2}\left(\overline{\delta p}^{n} + f^{\theta}(\overline{\delta p}^{n})\right)\right] + F^{\theta}\left[\frac{1}{2}\left(\overline{\delta p}^{n} + f^{\lambda}(\overline{\delta p}^{n})\right)\right],$$

Advantages:

- Inherently mass conservative (note: conservation does not necessarily imply accuracy!).
- Formulated in terms of one-dimensional operators.
- Preserves a constant for a non-divergent flow field (if the finite-difference approximation to divergence is zero).
- Preserves linear correlations between trace species (if shape-preservation filters are not applied)
- Has shape-preserving options.

# Namelist variables for *outer* operators

IORD: Scheme used for $F^{\lambda}$, JORD: Scheme used for $F^{\theta}$

Options for sub-grid-scale reconstruction (IORD, JORD = -2,1,2,3,4,5,6):

- -2 Piecewise linear (non shape-preserving), (van Leer, 1977).
- 1 Piecewise constant (Godunov, 1959).
- 2 Piecewise linear with shape-preservation constraint (van Leer, 1977).
- 3 Piecewise parabolic with shape-preservation constraint (Colella and Woodward, 1984).
- 4 Piecewise parabolic with shape-preservation constraint (Lin and Rood, 1996).
- 5 Piecewise parabolic with positive definite constraint (Lin and Rood, 1996).
- 6 Piecewise parabolic with quasi 'shape-preservation' constraint (Lin and Rood, 1996).

Defaults: IORD=JORD=4

# Namelist variables for *outer* operators

- In top layers operators are reduced to first order:

  $$\text{if } (\texttt{k} \leqslant \texttt{klev/8}) \; \texttt{IORD=JORD=1}$$

  E.g., for `klev=30` the operators are altered in the top 3 layers.

- The advective $f^{\lambda,\theta}$ (*inner*) operators are 'hard-coded' to 1st order. For a linear analysis of the consequences of using *inner* and *outer* operators of different orders see Lauritzen (2007).

# Adiabatic frictionless equations of motion

Hydrostatic equations of motion integrated over a Lagrangian layer

$$\begin{aligned}
\frac{\partial(\delta p)}{\partial t} &= -\nabla_h \cdot (\vec{v}_h \delta p), \\
\frac{\partial(\delta p q)}{\partial t} &= -\nabla_h \cdot (\vec{v}_h \delta p), \\
\frac{\partial \vec{v}_h}{\partial t} &= -(\zeta + f)\,\vec{k} \times \vec{v}_h - \nabla_h \kappa - \nabla_p \Phi, \\
\frac{\partial(\delta p \Theta)}{\partial t} &= -\nabla_h \cdot (\vec{v}_h \delta p \Theta)
\end{aligned}$$

The equations of motion are discretized using an Eulerian finite-volume approach.

# Adiabatic frictionless equations of motion

Hydrostatic equations of motion integrated over a Lagrangian layer

$$
\begin{aligned}
\overline{\delta p}^{n+1} &= \overline{\delta p}^{n} + F^{\lambda}\left[\frac{1}{2}\left(\overline{\delta p}^{n} + f^{\theta}(\overline{\delta p}^{n})\right)\right] + F^{\theta}\left[\frac{1}{2}\left(\overline{\delta p}^{n} + f^{\lambda}(\overline{\delta p}^{n})\right)\right], \\
\frac{\partial(\delta p q)}{\partial t} &= -\nabla_h \cdot (\vec{v}_h \delta p), \\
\frac{\partial \vec{v}_h}{\partial t} &= -(\zeta + f)\,\vec{k} \times \vec{v}_h - \nabla_h \kappa - \nabla_p \Phi, \\
\frac{\partial(\delta p \Theta)}{\partial t} &= -\nabla_h \cdot (\vec{v}_h \delta p \Theta)
\end{aligned}
$$

# Adiabatic frictionless equations of motion

Hydrostatic equations of motion integrated over a Lagrangian layer

$$\overline{\delta p}^{n+1} = \overline{\delta p}^{n} + F^{\lambda}\left[\frac{1}{2}\left(\overline{\delta p}^{n} + f^{\theta}(\overline{\delta p}^{n})\right)\right] + F^{\theta}\left[\frac{1}{2}\left(\overline{\delta p}^{n} + f^{\lambda}(\overline{\delta p}^{n})\right)\right],$$

$$\overline{\delta pq}^{n+1} = \text{super-cycled (discussed later)},$$

$$\frac{\partial \vec{v}_h}{\partial t} = -(\zeta + f)\,\vec{k} \times \vec{v}_h - \nabla_h \kappa - \nabla_p \Phi,$$

$$\frac{\partial(\delta p \Theta)}{\partial t} = -\nabla_h \cdot (\vec{v}_h \delta p \Theta)$$

# Adiabatic frictionless equations of motion

Hydrostatic equations of motion integrated over a Lagrangian layer

$$\overline{\delta p}^{n+1} = \overline{\delta p}^{n} + F^{\lambda}\left[\frac{1}{2}\left(\overline{\delta p}^{n} + f^{\theta}(\overline{\delta p}^{n})\right)\right] + F^{\theta}\left[\frac{1}{2}\left(\overline{\delta p}^{n} + f^{\lambda}(\overline{\delta p}^{n})\right)\right],$$

$$\overline{\delta p q}^{n+1} = \text{super-cycled (discussed later)},$$

$$\vec{v}_h^{n+1} = \vec{v}_h^{n} - \vec{\Gamma}^1\left[(\zeta + f)\,\vec{k}\times\vec{v}_h\right] - \nabla_h\left(\vec{\Gamma}^2\kappa\right) - \Delta t_{dyn}\widehat{P},$$

$$\frac{\partial(\delta p\Theta)}{\partial t} = -\nabla_h\cdot(\vec{v}_h\delta p\Theta)$$

- $\vec{\Gamma}^1$ is operator using combinations of $F^{\lambda,\theta}$ and $f^{\lambda,\theta}$ as components to approximate the time-volume-average of the vertical component of absolute vorticity. Similarly for $\vec{\Gamma}^2$ but for kinetic energy. $\nabla_h$ is simply approximated by finite differences. For details see Lin (2004).
- $\widehat{P}$ is a finite-volume discretization of the pressure gradient force (see Lin 1997 for details).

Hydrostatic equations of motion integrated over a Lagrangian layer

$$
\begin{aligned}
\overline{\delta p}^{n+1} &= \overline{\delta p}^{n} + F^{\lambda}\left[\frac{1}{2}\left(\overline{\delta p}^{n} + f^{\theta}(\overline{\delta p}^{n})\right)\right] + F^{\theta}\left[\frac{1}{2}\left(\overline{\delta p}^{n} + f^{\lambda}(\overline{\delta p}^{n})\right)\right],\\
\overline{\delta p q}^{n+1} &= \text{super-cycled (discussed later)},\\
\vec{v}_h^{n+1} &= \vec{v}_h^{n} - \vec{\Gamma}^{1}\left[(\zeta + f)\,\vec{k}\times\vec{v}_h\right] - \nabla_h\left(\vec{\Gamma}^{2}\kappa\right) - \Delta t_{dyn}\widehat{P},\\
\overline{\Theta\delta p}^{n+1} &= \overline{\Theta\delta p}^{n} + F^{\lambda}\left[\frac{1}{2}\left(\overline{\Theta\delta p}^{n} + f^{\theta}(\overline{\Theta\delta p}^{n})\right)\right] + F^{\theta}\left[\frac{1}{2}\left(\overline{\Theta\delta p}^{n} + f^{\lambda}(\overline{\Theta\delta p}^{n})\right)\right],
\end{aligned}
$$

# Adiabatic frictionless equations of motion

Hydrostatic equations of motion integrated over a Lagrangian layer

$$\overline{\delta p}^{n+1} = \overline{\delta p}^{n} + F^{\lambda}\left[\frac{1}{2}\left(\overline{\delta p}^{n} + f^{\theta}(\overline{\delta p}^{n})\right)\right] + F^{\theta}\left[\frac{1}{2}\left(\overline{\delta p}^{n} + f^{\lambda}(\overline{\delta p}^{n})\right)\right],$$

$$\overline{\delta p q}^{n+1} = \text{super-cycled (discussed later)},$$

$$\vec{v}_h^{n+1} = \vec{v}_h^{n} - \vec{\Gamma}^{1}\left[(\zeta + f)\,\vec{k}\times\vec{v}_h\right] - \nabla_h\left(\vec{\Gamma}^{2}\kappa\right) - \Delta t_{dyn}\widehat{P},$$

$$\overline{\Theta\delta p}^{n+1} = \overline{\Theta\delta p}^{n} + F^{\lambda}\left[\frac{1}{2}\left(\overline{\Theta\delta p}^{n} + f^{\theta}(\overline{\Theta\delta p}^{n})\right)\right] + F^{\theta}\left[\frac{1}{2}\left(\overline{\Theta\delta p}^{n} + f^{\lambda}(\overline{\Theta\delta p}^{n})\right)\right],$$

- No explicit diffusion operators in equations (so far!).
- Implicit diffusion trough shape-preservation constraints in $F$ and $f$ operators.
- CAM-FV has ‘control’ over vorticity at the grid scale through implicit diffusion in the operators $F$ and $f$ but it does not have explicit control over divergence near the grid scale.

# Adiabatic frictionless equations of motion

Hydrostatic equations of motion integrated over a Lagrangian layer

$$\overline{\delta p}^{n+1} = \overline{\delta p}^{n} + F^{\lambda}\left[\frac{1}{2}\left(\overline{\delta p}^{n} + f^{\theta}(\overline{\delta p}^{n})\right)\right] + F^{\theta}\left[\frac{1}{2}\left(\overline{\delta p}^{n} + f^{\lambda}(\overline{\delta p}^{n})\right)\right],$$

$$\overline{\delta pq}^{n+1} = \text{super-cycled (discussed later)},$$

$$\vec{v}_h^{n+1} = \vec{v}_h^{n} - \vec{\Gamma}^{1}\left[(\zeta + f)\,\vec{k} \times \vec{v}_h\right] - \nabla_h\left(\vec{\Gamma}^{2}\kappa\right) - \Delta t_{dyn}\widehat{P} + \Delta t_{dyn}\nabla_h(\nu D),$$

$$\overline{\Theta\delta p}^{n+1} = \overline{\Theta\delta p}^{n} + F^{\lambda}\left[\frac{1}{2}\left(\overline{\Theta\delta p}^{n} + f^{\theta}(\overline{\Theta\delta p}^{n})\right)\right] + F^{\theta}\left[\frac{1}{2}\left(\overline{\Theta\delta p}^{n} + f^{\lambda}(\overline{\Theta\delta p}^{n})\right)\right],$$

- No explicit diffusion operators in equations.
- Implicit diffusion trough shape-preservation constraints in $F$ and $f$ operators.
- The above discretization leads to 'control' over vorticity at the grid scale through implicit diffusion but no explicit control over divergence.
- Add divergence damping term to momentum equations.

Divergence damping uses explicit time-stepping; model will be unstable for too large divergence damping coefficients

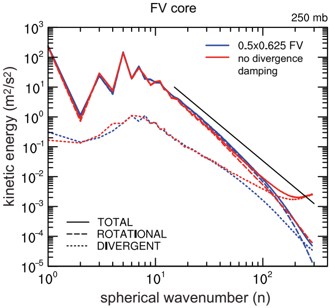


Figure: Solid black line shows $k^{-3}$ slope. Plot courtesy of David L. Williamson.

Without divergence damping there is a spurious accumulation of total kinetic energy associated with divergent modes near the grid scale.

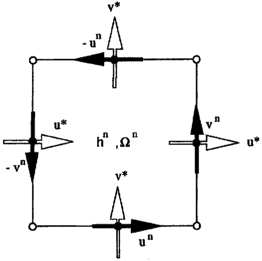


Figure from Lin and Rood (1997).

Definition of Arakawa C and D horizontal staggering (Arakawa and Lamb, 1977):

- C: Velocity components at the center of cell faces and orthogonal to cell faces and mass variables at the cell center. Natural choice for mass-flux computations when using Lin and Rood (1996) scheme.
- D: Velocity components parallel to cell faces and mass variables at the cell center. Natural choice for computing the circulation of vorticity ($\frac{\partial v}{\partial x} - \frac{\partial u}{\partial y}$).

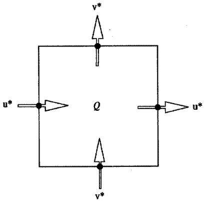


Figure from Lin and Rood (1997).

- For the flux- and advection operators ($F$ and $f$, respectively) in the Lin and Rood (1996) scheme the time-centered advective winds $(u^*, v^*)$ for the cell faces are needed:
- An option: Extrapolate winds (as in semi-Lagrangian models) $\Rightarrow$ Noise near steep topography (Lin and Rood, 1997).

- Instead, the equations of motion are integrated forward in time for $\frac{1}{2}\Delta t_{dyn}$ using a $C$ grid horizontal staggering.
- These C-grid winds $(u^*, v^*)$ are then used for the 'full' time-step update (everything else from the $C$-grid forecast is 'thrown away').
- The 'full' time-step update is performed on a $D$-grid.
- For a linear stability analysis of the 'CD'-grid approach see Skamarock (2008).

# Vertical remapping

- CAM-FV uses a Lagrangian ('floating') vertical coordinate $\xi$.
- $\xi$ is retained *ksplit* dynamics time-steps $\Delta t_{dyn}$.
- Hereafter the prognostic variables are remapped to the Eulerian vertical grid $\eta$ (the vertical remapping is performed using an energy conserving method, see Lin 2004).
- *ksplit* is set in `namelist`:

```
-nsplit ksplit
```

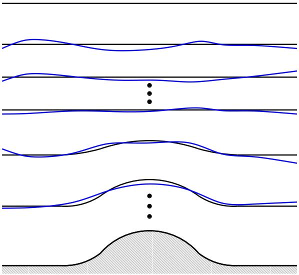

- The 'physics time-step is set in the `namelist`:

```
-dtime Δt,
```

  where $\Delta t$ s is given in seconds.
- At every physics time-step $\Delta t$ the variables are remapped in the vertical as described above.
- So the dynamics time-step $\Delta t_{dyn}$ is controlled with *ksplit* and $\Delta t$ in the `namelist`:

$$\Delta t = ksplit \times \Delta t_{dyn}.$$

(in CAM5 there is also an option to vertical remap more often and it changes $\Delta t$)

# Vertical remapping

- CAM-FV uses a Lagrangian ('floating') vertical coordinate $\xi$.
- $\xi$ is retained *ksplit* dynamics time-steps $\Delta t_{dyn}$.
- Hereafter the prognostic variables are remapped to the Eulerian vertical grid $\eta$ (the vertical remapping is performed using an energy conserving method, see Lin 2004).
- *ksplit* is set in `namelist`:

```
-nsplit ksplit
```

- Default setting for the 1.9×2.5 resolution is $ksplit = 4$ and $\Delta t = 1800s$ (so $\Delta t_{dyn} = 450s$).
- *ksplit* is usually chosen based on stability.
- (meridians are converging towards the poles) To stabilize the model (and reduce noise) FFT filters are applied along latitudes north and south of the tropics.

# Super-cycling (also referred to as sub-cycling) of tracers

- Continuity equation for air is coupled with momentum and thermodynamic equations:

# Super-cycling (also referred to as sub-cycling) of tracers

- Continuity equation for air is coupled with momentum and thermodynamic equations:
  - thermodynamic variables and other prognostic variables feed back on the velocity field

# Super-cycling (also referred to as sub-cycling) of tracers

- Continuity equation for air is coupled with momentum and thermodynamic equations:
  - thermodynamic variables and other prognostic variables feed back on the velocity field
  - which, in turn, feeds back on the solution to the continuity equation.

# Super-cycling (also referred to as sub-cycling) of tracers

- Continuity equation for air is coupled with momentum and thermodynamic equations:
  - thermodynamic variables and other prognostic variables feed back on the velocity field
  - which, in turn, feeds back on the solution to the continuity equation.
  - Hence the continuity equation for air can not be solved in isolation and one must obey the maximum allowable time-step restrictions imposed by the fastest waves in the system.

# Super-cycling (also referred to as sub-cycling) of tracers

- Continuity equation for air is coupled with momentum and thermodynamic equations:
  - thermodynamic variables and other prognostic variables feed back on the velocity field
  - which, in turn, feeds back on the solution to the continuity equation.
  - Hence the continuity equation for air can not be solved in isolation and one must obey the maximum allowable time-step restrictions imposed by the fastest waves in the system.
- The passive tracer transport equation can be solved in isolation given prescribed winds and air densities, and is therefore not susceptible to the time-step restrictions imposed by the fastest waves in the system.

# Super-cycling (also referred to as sub-cycling) of tracers

- Continuity equation for air is coupled with momentum and thermodynamic equations:
  - thermodynamic variables and other prognostic variables feed back on the velocity field
  - which, in turn, feeds back on the solution to the continuity equation.
  - Hence the continuity equation for air can not be solved in isolation and one must obey the maximum allowable time-step restrictions imposed by the fastest waves in the system.
- The passive tracer transport equation can be solved in isolation given prescribed winds and air densities, and is therefore not susceptible to the time-step restrictions imposed by the fastest waves in the system.
- For efficiency: Use longer time-step for tracers than for air.

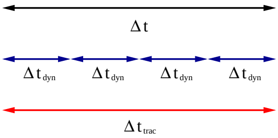


$\Delta t_{trac}$ is time-step of the tracers. Specified in terms of `nspltrac` (default for $1.9 \times 2.5$ resolution is `nspltrac=1`).

Leads to a major 'speed-up' of dynamics.

# Free-stream preserving 'super-cycling' of tracers with respect to air ρ

Simply solving the tracer continuity equation for $\overline{q\delta p}^{n+1}$ using $\Delta t_{trac}$ will lead to inconsistencies. Why?

Continuity equation for air $\delta p$

$$\frac{\partial \delta p}{\partial t} + \nabla \cdot (\delta p\, \vec{v}_h) = 0, \tag{7}$$

and a tracer with mixing ratio $q$

$$\frac{\partial (\delta p\, q)}{\partial t} + \nabla \cdot (\delta p\, q\, \vec{v}_h) = 0, \tag{8}$$

For $q = 1$ equation (8) reduces to (7). If this is satisfied in the numerical discretizations, the scheme is 'free-stream' preserving.

Solving (8) with $q = 1$ using $\Delta t_{trac}$ will NOT produce the same solution as solving (7) `nspltrac` times using $\Delta t_{dyn}$!

# Graphical illustration of ‘free stream’ preserving transport of tracers

Assume no flux through east cell wall.

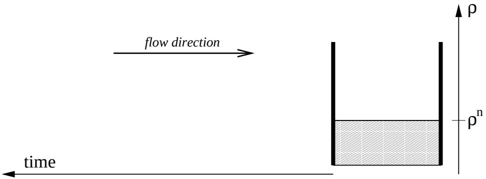


- Solve continuity equation for air $\rho = \delta p$ together with momentum and thermodynamics equations.

# Graphical illustration of ‘free stream’ preserving transport of tracers

Assume no flux through east cell wall.

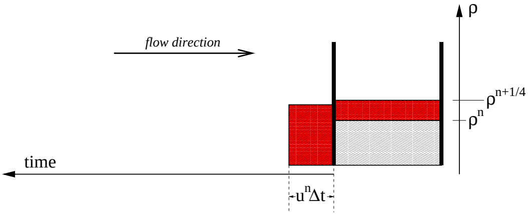


- Solve continuity equation for air $\rho = \delta p$ together with momentum and thermodynamics equations.

# Graphical illustration of ‘free stream’ preserving transport of tracers

Assume no flux through east cell wall.

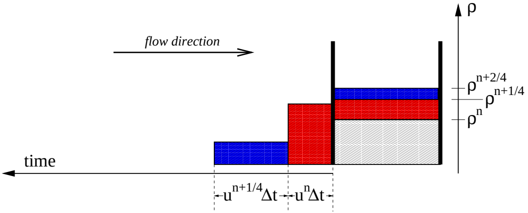


- Solve continuity equation for air $\rho = \delta p$ together with momentum and thermodynamics equations.
- Repeat *ksplit* times

# Graphical illustration of ‘free stream’ preserving transport of tracers

Assume no flux through east cell wall.

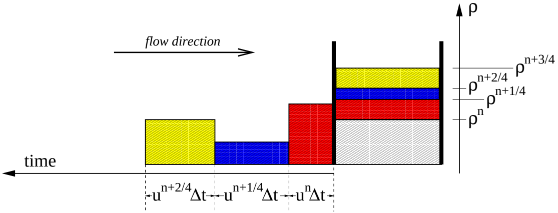


- Solve continuity equation for air $\rho = \delta p$ together with momentum and thermodynamics equations.
- Repeat *ksplit* times

# Graphical illustration of 'free stream' preserving transport of tracers

Assume no flux through east cell wall.

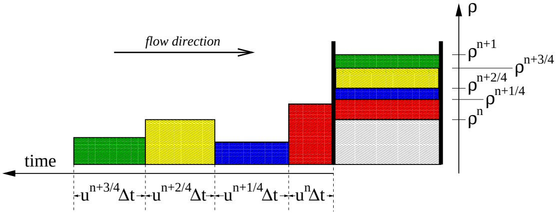


- Solve continuity equation for air $\rho = \delta p$ together with momentum and thermodynamics equations.
- Repeat *ksplit* times

# Graphical illustration of 'free stream' preserving transport of tracers

Assume no flux through east cell wall.

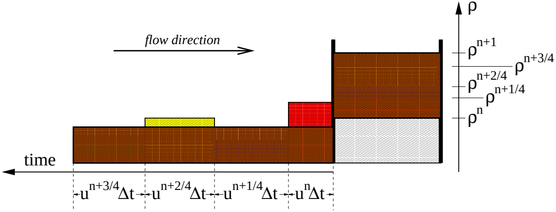


- Solve continuity equation for air $\rho = \delta p$ together with momentum and thermodynamics equations.
- Repeat *ksplit* times
- Brown area = average flow of mass through cell face.
- Compute time-averaged value of $q$ across brown area using Lin and Rood (1996) scheme: $\overline{\overline{<q>}}$.
- Forecast for tracer is: $\overline{\overline{<q>}} \times \sum_{i=1}^{ksplit} \delta p^{n+i/ksplit}$
- Yields 'free stream' preserving solution!

- CAM-FV has a very efficient and quite consistent treatment of the tracers.
- This is very important: Number of trace species in climate models are increasing and accounts for most of the computational ‘work’ in the dynamical core.

# CAM-FV performance

- CAM-FV has a very efficient and quite consistent treatment of the tracers.
- This is very important: Number of trace species in climate models are increasing and accounts for most of the computational 'work' in the dynamical core.
- Rasch et al. (2006) did a comprehensive study of the characteristics of atmospheric transport using three dynamical cores in CAM (CAM-FV, CAM-EUL, CAM-SL; acronyms defined later):

  The results from this study favor use of the CAM-FV core for tracer transport. Unlike the others, CAM-FV

  - is inherently conservative
  - less diffusive (e.g. maintains strong gradients better)
  - maintains the nonlinear relationships among variables required by thermodynamic and mass conservation constraints more accurately.

# CAM-FV performance

- CAM-FV has a very efficient and quite consistent treatment of the tracers.
- This is very important: Number of trace species in climate models are increasing and accounts for most of the computational 'work' in the dynamical core.
- Rasch et al. (2006) did a comprehensive study of the characteristics of atmospheric transport using three dynamical cores in CAM (CAM-FV, CAM-EUL, CAM-SL; acronyms defined later):

  The results from this study favor use of the CAM-FV core for tracer transport. Unlike the others, CAM-FV

  - is inherently conservative
  - less diffusive (e.g. maintains strong gradients better)
  - maintains the nonlinear relationships among variables required by thermodynamic and mass conservation constraints more accurately.

However, with respect to 'meteorology' CAM-FV needs higher horizontal resolution to produce results equivalent to those produced using the spectral transform dynamical core in CAM (CAM-EUL). See Williamson (2008) for details.

# Excessive polar night jet when increasing horizontal resolution

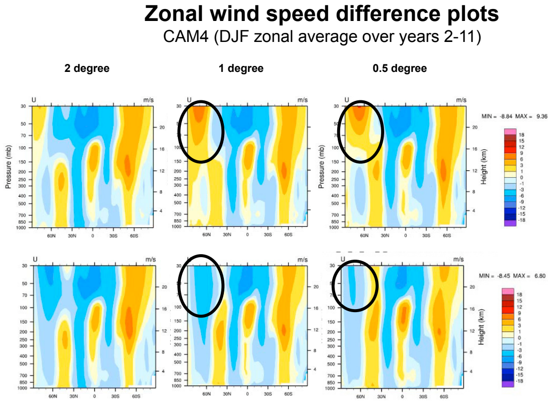


Figure:

- $1^{st}$ row: Difference between zonal wind speed and observations (NCEP) during Northern winter using default CAM.
- $2^{nd}$ row: Same as $1^{st}$ row but for default CAM + $\nabla^2$ damping of velocity components near model top

Laplacian damping of wind components near model top alleviates this problem (optional in CAM5; controlled with namelist variable `div24del2flag`)

More details: Lauritzen et al. (2011)

# Noise in divergence field aligned with grid

Instantaneous divergence around 200 $hPa$ in units of $1e10^{-5}/s$

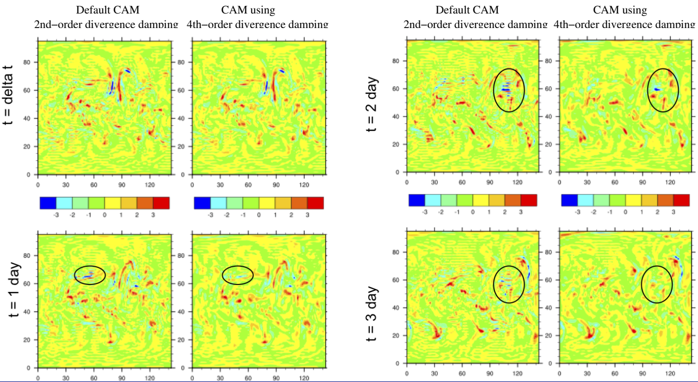


Divergence associated with "physical" features seem preserved while grid-scale noise is alleviated

- The noise can be reduced by increasing the divergence damping coefficient (at the cost of excessive damping in terms of total kinetic energy spectra analysis) or using $4^{th}$-order divergence damping (option added to CAM5; namelist variable `div24del2flag`)
- $4^{th}$-order divergence damping significantly reduces noise when running CAM in 'weather forecast-mode' using DART (DART = Data Assimilation Research Testbed). More details: Lauritzen et al. (2011)

# Idealized settings for CAM

- ADIABATIC: No physics. See example of application in Jablonowski and Williamson (2006).

- IDEAL_PHYS: Held-Suarez test case (Held and Suarez, 1994):
  - Simple Newtonian relaxation of the temperature field to a zonally symmetric state
  - Rayleigh damping of low-level winds representing boundary-layer friction

- AQUA_PLANET: Ocean only planet with zonally symmetric SST-forcing using 'full' physics package (Neale and Hoskins, 2000). See example of application in Williamson (2008).

- CAM-EUL (Collins et al., 2004):
  - Based on the spectral transform method
  - Semi-implicit time-stepping
  - Tracer transport with non-conservative semi-Lagrangian scheme ('fixers' restore formal mass-conservation)
- CAM-SL (Collins et al., 2004): Same as CAM-EUL but based entirely on a semi-Lagrangian discretization.
- CAM-SE (Evans et al., 2012): Spectral Elements
  - A dynamical core in HOMME (High-Order Method Modeling Environment, Thomas and Loft 2005).
  - Based on local spectral element method
  - For each element: Mass-conservative to machine precision and total energy conservative to the truncation error of the time integration scheme
  - Discretized on cubed-sphere
  - Highly scalable! (has been run on over 170.000 cores)
  - Currently being considered for default dynamical core in the next release of CAM5

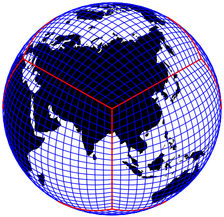

# Interested in numerical methods for global models?

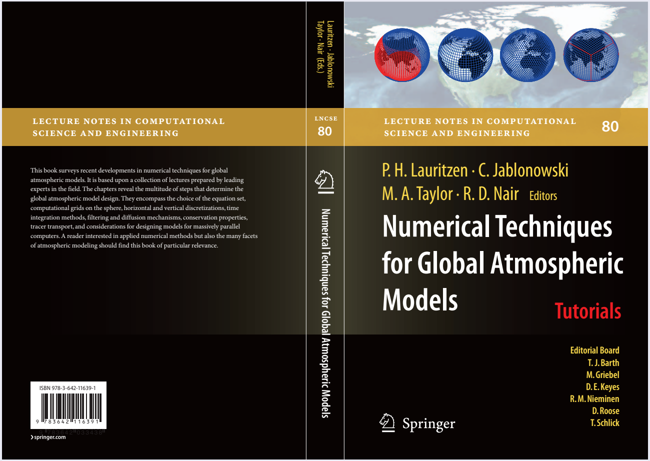


- Book based on the lectures given at the 2008 NCAR ASP (Advance Study Program) Summer Colloquium.
- 16 Chapters; authors include J.Thuburn, J.Tribbia, D.Durran, T.Ringler, W.Skamarock, R.Rood, J.Dennis, Editors, ... Foreword by D. Randall
- More details at: http://www.cgd.ucar.edu/cms/pel/colloquium.html and http://www.cgd.ucar.edu/cms/pel/lncse.html

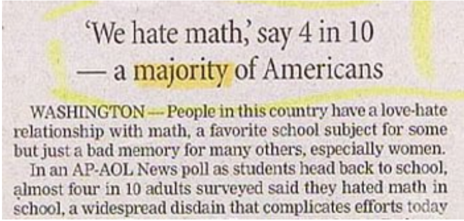

'We hate math,' say 4 in 10 — a majority of Americans

WASHINGTON — People in this country have a love-hate relationship with math, a favorite school subject for some but just a bad memory for many others, especially women.
In an AP-AOL News poll as students head back to school, almost four in 10 adults surveyed said they hated math in school, a widespread disdain that complicates efforts today

**'In mathematics you don't understand things. You just get used to them.'**
**- John von Neumann**

# Questions?

References

Arakawa, A. and Lamb, V. R. (1977). Computational design and the basic dynamical processes of the UCLA general circulation model. *Methods in Computational Physics*, 17:172–265.

Colella, P. and Woodward, P. R. (1984). The piecewise parabolic method (PPM) for gas-dynamical simulations. *J. Comput. Phys.*, 54:174–201.

Collins, W. D., Rasch, P. J., Boville, B. A., Hack, J. J., McCaa, J. R., Williamson, D. L., Kiehl, J. T., and Briegleb, B. (2004). Description of the NCAR Community Atmosphere Model (CAM 3.0). NCAR Tech. Note, NCAR/TN-464+STR.

Evans, K., Lauritzen, P. H., Mishra, S., Neale, R., Taylor, M. A., and Tribbia, J. J. (2012). AMIP simulations wiht the CAM4 spectral element dynamical core. *J. Climate*. revising.

Godunov, S. K. (1959). A difference scheme for numerical computation of discontinuous solutions of equations in fluid dynamics. *Math. Sb.*, 47:271. Also: Cornell Aero. Lab. translation.

Held, I. M. and Suarez, M. J. (1994). A proposal for the intercomparison of the dynamical cores of atmospheric general circulation models. *Bull. Amer. Meteor. Soc.*, 75:1825–1830.

Jablonowski, C. and Williamson, D. L. (2006). A baroclinic instability test case for atmospheric model dynamical cores. *Q. J. R. Meteorol. Soc.*, 132:2943–2975.

Lauritzen, P. H. (2007). A stability analysis of finite-volume advection schemes permitting long time steps. *Mon. Wea. Rev.*, 135:2658–2673.

Lauritzen, P. H., Mirin, A., Truesdale, J., Raeder, K., Anderson, J., Bacmeister, J., and Neale, R. B. (2011). Implementation of new diffusion/filtering operators in the CAM-FV dynamical core. *International Journal of High Performance Computing Applications*.

Lin, S. J. (1997). Ti: A finite-volume integration method for computing pressure gradient force in general vertical coordinates. *Quart. J. Roy. Meteor. Soc.*, 123:1749–1762.

Lin, S.-J. (2004). A 'vertically Lagrangian' finite-volume dynamical core for global models. *Mon. Wea. Rev.*, 132:2293–2307.

Lin, S. J. and Rood, R. B. (1996). Multidimensional flux-form semi-Lagrangian transport schemes. *Mon. Wea. Rev.*, 124:2046–2070.

Lin, S.-J. and Rood, R. B. (1997). An explicit flux-form semi-Lagrangian shallow-water model on the sphere. *Q.J.R.Meteorol.Soc.*, 123:2477–2498.

Machenhauer, B., Kaas, E., and Lauritzen, P. H. (2009). Finite volume methods in meteorology, in: R. Temam, J. Tribbia, P. Ciarlet (Eds.), Computational methods for the atmosphere and the oceans. *Handbook of Numerical Analysis*, 14. Elsevier, 2009, pp.3-120.

Neale, R. B. and Hoskins, B. J. (2000). A standard test for AGCMs and their physical parameterizations. i: The proposal. *Atmos. Sci. Letters*, 1:101–107.

Rasch, P. J., Coleman, D. B., Mahowald, N., Williamson, D. L., Lin, S. J., Boville, B. A., and Hess, P. (2006). Characteristics of atmospheric transport using three numerical formulations for atmospheric dynamics in a single GCM framework. *J. Climate*, 19:2243–2266.

Skamarock, W. C. (2008). A linear analysis of the NCAR CCSM finite-volume dynamical core. *Mon. Wea. Rev.*, 136:2112–2119.

Thomas, S. J. and Loft, R. D. (2005). The NCAR spectral element climate dynamical core: Semi-implicit Eulerian formulation. *J. Sci. Comput.*, 25:307–322.

Thuburn, J. (2008). Some conservation issues for the dynamical cores of NWP and climate models. *J. Comput. Phys.*, 227:3715 – 3730.

Thuburn, J. (2011). Some basic dynamics relevant to the design of atmospheric model dynamical cores, in: P.H. Lauritzen, R.D. Nair, C. Jablonowski, M. Taylor (Eds.), Numerical techniques for global atmospheric models. *Lecture Notes in Computational Science and Engineering, Springer*, 80.

van Leer, B. (1977). Towards the ultimate conservative difference scheme. IV: A new approach to numerical convection. *J. Comput. Phys.*, 23:276–299.

Williamson, D. L. (2002). Time-split versus process-split coupling of parameterizations and dynamical core. *Mon. Wea. Rev.*, 130:2024–2041.

Williamson, D. L. (2008). Equivalent finite volume and Eulerian spectral transform horizontal resolutions established from aqua-planet simulations. *Tellus*, 60:839–847.

Williamson, D. L. and Olson, J. G. (2003). Dependence of aqua-planet simulations on time step. *Q. J. R. Meteorol. Soc.*, 129(591):2049–2064.